ChemComm

COMMUNICATION

High catalytic activity and stability of nickel sulfide and cobalt sulfide hierarchical nanospheres on the counter electrodes for dye-sensitized solar cells†

Cite this: *Chem. Commun.*, 2014, 50, 4824

Received 7th January 2014,
Accepted 17th March 2014

DOI: 10.1039/c4cc00001c

www.rsc.org/chemcomm

Jie Yang,[ab] Chunxiong Bao,[ab] Kai Zhu,[c] Tao Yu,*[ab] Faming Li,[ab] Jianguo Liu,[ad] Zhaosheng Li[ad] and Zhigang Zou[abcd]

In situ **grown nickel sulfide and cobalt sulfide hierarchical nanospheres on F-doped SnO_2 (FTO) substrates exhibited comparable catalytic activities to sputtering Pt on the counter electrodes for dye-sensitized solar cells (DSSCs). The fresh cells with the nickel sulfide and cobalt sulfide on the counter electrodes could reach power conversion efficiencies of 6.81% and 6.59% respectively, approaching an efficiency of 6.85% based on the sputtering Pt counter electrode. Both nickel sulfide and cobalt sulfide counter electrodes could maintain the cell's relatively high performance in the long-term stability test in 504 hours.**

Dye-sensitized solar cells (DSSCs) have been considered as the potential next-generation photovoltaic devices due to their acceptable efficiencies, low cost of materials, simple fabrication procedures and so on.[1–3] One of the most important components in a DSSC is the counter electrode (CE) whose main role is to collect the electrons from the external circuit and catalyze the reduction of I_3^- to I^- at the CE/electrolyte interface. Therefore, a high electrical conductivity for the electrons collecting,[4,5] a large specific surface area for the CE/electrolyte contact[6–9] and a high catalytic activity for the reaction of I_3^- to I^- are supposed to be preferred characteristics for the ideal CEs in DSSCs. In this respect, Pt sheets have been recognized as suitable counter electrodes because of their high catalytic activity and stability. However, Pt is an expensive and scarce metal, which inevitably influences large-scale manufacturing of the DSSCs containing expensive Pt. Therefore, the Pt-free materials used as DSSCs' counter electrodes are important for the future industrial application of DSSCs.

The nickel sulfides and cobalt sulfides have high catalytic activities for the redox couples I^-/I_3^- in DSSCs. In 2009, CoS electrodeposited on the flexible ITO/PEN substrate showed comparable catalytic activity to Pt as the counter electrodes in DSSCs, which opens up the way to exploring more transition metal sulfides.[10] In 2011, Sun *et al.* found that NiS counter electrode electrodeposited using a potential reversal technique showed high catalytic activity for the reduction of I_3^- to I^-.[11]

It is well known that a high specific surface area is beneficial for increasing the active sites. In the past years, the hierarchical nanostructures have been applied in both of the working electrodes[12,13] and the counter electrodes[14–16] in DSSCs due to a lot of advantages such as the large specific surface area providing large electrode/electrolyte interface contact, the accessible inner surface for electrolyte filling and so on. Hierarchical Pt aggregates have been deposited on a thin TiO_2 layer modified ITO substrate as the counter electrode for the flexible DSSC by Fu *et al.*[14] Wang *et al.* has reported that hierarchical cobalt sulfide spindles in the counter electrodes in DSSCs showed high catalytic activity.[15] However, the fabrication procedures of hierarchical structure were relatively complicated. *In situ* growth has been considered to be a very simple method for fabrication of thin films on the substrates.[17] Our previous work employed *in situ* growth procedures in the preparation of the vertically oriented $CuInS_2$ nanosheet thin films with high catalytic activity as counter electrodes in DSSCs.[18] However, indium is an expensive and scarce metal. Herein, we present a one-step solvothermal process for *in situ* preparation of highly stable hierarchical nickel sulfide and cobalt sulfide nanospheres without any scarce elements, which increase the catalytic sites for the catalytic reaction of the redox couple I^-/I_3^-. Meanwhile, DSSCs assembled with the nickel sulfide and cobalt sulfide counter electrodes were further investigated by long-term stability tests and showed comparable stability to Pt in 504 hours, which are the potential materials for future manufacturing.

The nickel sulfide and cobalt sulfide thin films were grown *in situ* on the FTO conductive glass using a solvothermal method without any post-treatment. The experimental details are shown in the ESI.† The SEM image in Fig. 1a shows that the nickel sulfide nanospheres are distributed uniformly on the FTO glass. The inset of Fig. 1a shows the higher resolution SEM image of the nickel sulfide nanospheres, and shows that the nickel sulfide nanospheres with sizes of about 200 nm are composed of smaller nanoparticles. Fig. 1c and its

[a] *National Laboratory of Solid State Microstructures, Nanjing University, Nanjing 210093, P. R. China. E-mail: yutao@nju.edu.cn*
[b] *Eco-Materials and Renewable Energy Research Center (ERERC), Department of Physics, Nanjing University, Nanjing 210093, P. R. China*
[c] *Kunshan Innovation Institute of Nanjing University, Kunshan 215347, P. R. China*
[d] *Department of Materials Science and Engineering, Nanjing University, Nanjing, 210093, P. R. China*

† Electronic supplementary information (ESI) available. See DOI: 10.1039/c4cc00001c

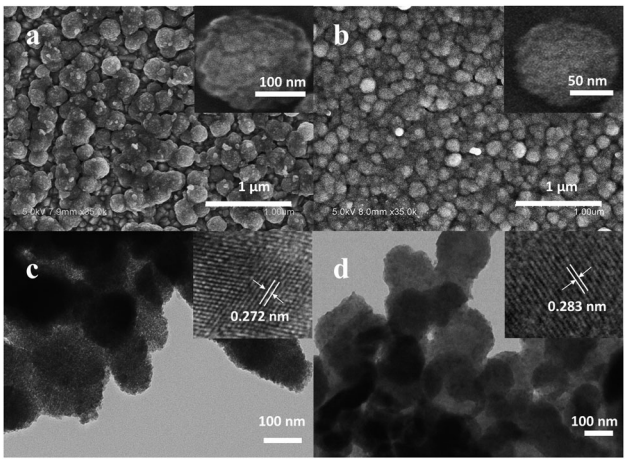

Fig. 1 The SEM image of hierarchical nickel sulfide (a) and cobalt sulfide (b) nanospheres with high resolution SEM inset. The TEM image of nickel sulfide (c) and cobalt sulfide (d) nanospheres with high solution TEM images inset.

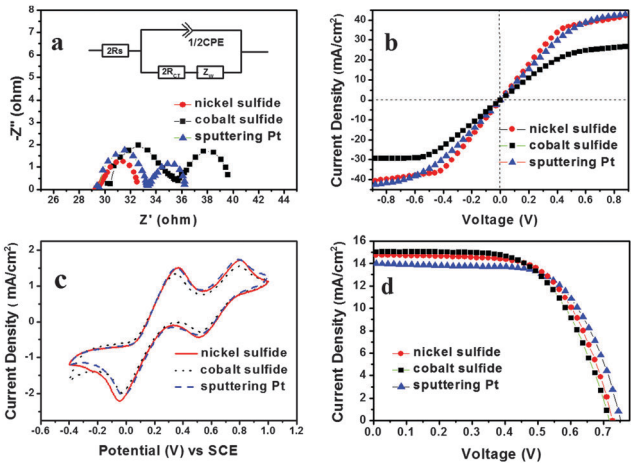

Fig. 2 The EIS Nyquist plots (a), polarization curves (b) and CV curves (c) of the nickel sulfide, cobalt sulfide and sputtering Pt counter electrodes. (d) The *J–V* curves of different DSSCs integrated with the same photoanode and the nickel sulfide, cobalt sulfide and sputtering Pt as counter electrodes.

inset show TEM images of nickel sulfide nanospheres which demonstrate that the nanospheres are composed of crystalline grains with a smaller size. Fig. 1b and d show that the morphologies of the cobalt sulfide nanospheres are almost the same as those of the nickel sulfide nanospheres. The SEM and TEM images indicate that both of the materials present hierarchical nanospheres structures with high surface roughness. The BET tests were undertaken on the films grown *in situ* on the FTO substrates. Unfortunately, we could not get the data for surface areas because the films were too thin to meet the lowest requirement in the BET tests.

From the HRTEM image inset in Fig. 1c and d we can measure the lattice spacing of the nickel sulfide and cobalt sulfide crystalline grain to be about 0.272 nm and 0.283 respectively, which corresponds to the (222) lattice plane spacing of Ni_3S_4 and the (211) lattice plane spacing of Co_3S_4. The result is in accordance with XRD data in Fig. S1 (ESI†). However, the EDS and XPS results shown in Fig. S2 (ESI†) indicate that the atomic ratio of sulfur to metal was not 4 : 3, which demonstrates that there are some other phases or amorphous nickel sulfide or cobalt sulfide in the nanospheres besides Ni_3S_4 and Co_3S_4.

Electrochemical impedance spectroscopy (EIS) is widely applied in the investigation of the electrochemical behaviour of the counter electrodes.[19–21] Fig. 2a shows the Nyquist plots of the corresponding symmetrical cells with the equivalent circuit in the inset. The simulated data from the EIS spectra are summarized in Table 1. The nickel sulfide and cobalt sulfide counter electrodes show quite small R_{ct} values of 0.43 Ω cm^2 and 0.75 Ω cm^2 respectively, which are comparable to that of sputtering Pt (0.56 Ω cm^2), indicating the catalytic activities of the nickel sulfide, cobalt sulfide nanospheres are comparable to that of sputtering Pt. The similar serial resistances R_s listed in Table 1 indicate that the electrical conductivities of nickel sulfide and cobalt sulfide film are comparable to that of sputtering Pt.

Polarization curves and cyclic voltammetry (CV) were used to further demonstrate the catalytic activity of the counter electrodes. From the polarization curves in Fig. 2b, the slope values at 0 V of nickel sulfide and cobalt sulfide counter electrodes are close to that of sputtering Pt, indicating that the catalytic activities of nickel sulfide and cobalt sulfide counter electrodes are comparable to that of sputtering Pt, which corresponds to the EIS data. From the polarization curves, the values of the limiting diffusion current density of the symmetrical cells assembled using nickel sulfide, cobalt sulfide and the sputtering Pt electrodes respectively range from 30 mA cm^{-2} to 40 mA cm^{-2}, which are much larger than the short-circuit current of the DSSCs assembled using the three counter electrodes shown in Fig. 2d. From our previous research on the maximum performance of the counter electrodes, we can see that the three counter electrodes exhibit no obvious negative effects on the assembled DSSCs.[22] CV curves in Fig. 2c all show two pairs of redox peaks. The two redox peaks at more negative potentials correspond to the reaction of

$$3I^- \leftrightarrow I_3^- + 2e^- \quad (1)$$

The cathodic peak current densities (I_{pc}) indicate the catalytic activities of the CEs for I_3^- reduction in DSSCs. The nickel sulfide and cobalt sulfide thin films show comparable I_{pc} to that of the sputtering Pt, demonstrating that nickel sulfide and cobalt sulfide counter electrodes possess comparable catalytic activities to the sputtering Pt.

The *J–V* curves of integrated DSSCs based on nickel sulfide and cobalt sulfide counter electrodes are shown in Fig. 2d. The detailed photovoltaic parameters are summarized in Table 1. From Fig. 2d, the assembled DSSCs based on the nickel sulfide and cobalt sulfide thin film reach power conversion efficiencies

Table 1 Photovoltaic performance, EIS parameters of the CEs with nickel sulfide, cobalt sulfide nanospheres and sputtering Pt

CE	V_{oc} (V)	J_{sc} (mA cm^{-2})	FF (%)	PCE (%)	R_{ct} (Ω cm^2)	R_s (Ω cm^2)	CPE (μF cm^{-2})
Nickel sulfide	0.73	14.70	63.50	6.81	0.43	4.18	10.9
Cobalt sulfide	0.72	15.03	61.00	6.59	0.75	4.30	18.2
Sputtering Pt	0.75	14.00	65.24	6.85	0.56	4.20	17.7

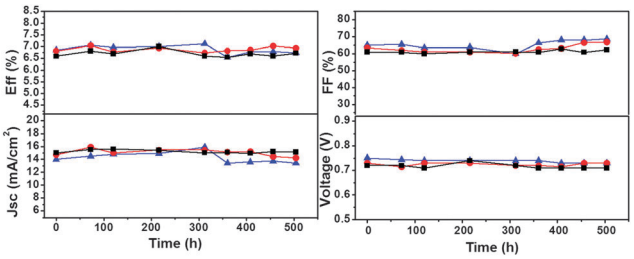

Fig. 3 Photovoltaic parameters variations of the DSSCs assembled with nickel sulfide (—●—), cobalt sulfide (–■–) and sputtering Pt (—▲—) as counter electrodes subjected to aging for 504 hours.

of 6.81% and 6.59% on the first day, which are comparable to that of sputtering Pt (6.85%). The high performances of nickel sulfide and cobalt sulfide counter electrodes result from their high catalytic activities and electrical conductivities as well as their rough surface and accessible inner surface for electrolyte filling.

Long-term stability is an important factor for device industrialization. The sensitizer, electrolyte and sealant have been considered as key factors for a long service life of DSSCs.[23–25] Although some reports have claimed that the Pt counter electrodes are at the risk of corrosion in the triiodide-containing solutions to generate platinum iodides such as PtI_4, Pt counter electrodes are more stable than the above-mentioned factors.[26] Long-term stability of the DSSCs assembled using nickel sulfide, cobalt sulfide and sputtering Pt in 504 hours are shown in Fig. 3. From the variation of Eff, J_{sc}, V_{oc} and FF of the DSSCs during 504 hours, we can see that the performances of the DSSCs stayed stable and showed no obvious degradation. The CV curves of each counter electrode for 50 cycles were further obtained to investigate the stability of the CEs. The variations of the three counter electrodes are shown in Fig. S3 (ESI†). The photovoltaic parameters and CV data demonstrated that nickel sulfide and cobalt sulfide counter electrodes had good stability compared to Pt. It is worth mentioning that, during the 504 hours, the highest power conversion efficiencies of nickel sulfide, cobalt sulfide and sputtering Pt cells were 7.02%, 7% and 7.12% respectively.

In summary, the nickel sulfide and cobalt sulfide hierarchical nanospheres counter electrodes were fabricated using a facile one-step *in situ* solvothermal method. The introduction of the hierarchical structure to the counter electrodes lead to a large interface contact between the electrolyte and the nickel sulfide, cobalt sulfide counter electrodes, accessible electrolyte filling in the counter electrode and good electrode conductivity, which is beneficial for the catalytic reaction of the I^-/I_3^-. The as-synthesized nickel sulfide and cobalt sulfide thin films were characterized using various electrochemical methods and showed comparable catalytic activities as counter electrodes to sputtering Pt. The power conversion efficiencies of the DSSCs using nickel sulfide (6.85%) and cobalt sulfide (6.59%) thin films as the counter electrodes were comparable to that using sputtering Pt (6.81%). The DSSCs assembled with nickel sulfide and cobalt sulfide counter electrodes showed quite high stability during 504 h of aging at room temperature without illumination.

We are thankful for the financial support from the National Natural Science Foundation of China (11174129, 61377051 and 51272102), the National Basic Research Program of China (2011CB933303 and 2013CB632404), the Jiangsu Provincial Science and Technology Research Program (BK2011056, BE2012089 and BK20130053). We thank Dr Hao Gao and Dr Zhiqiang Wang for their information discussions and experimental and technical assistance.

Notes and references

1 B. O'Regan and M. Grätzel, *Nature*, 1991, **353**, 737–740.
2 M. Grätzel, *Nature*, 2001, **414**, 338–344.
3 A. Yella, H. W. Lee, H. N. Tsao, C. Yi, A. K. Chandiran, M. d. Khaja Nazeeruddin, E. W. G. Diau, C. Y. Yeh, S. M. Zakeeruddin and M. Grätzel, *Science*, 2011, 629–634.
4 Y. Saito, T. Kitamura, Y. Wada and S. Yanagida, *Chem. Lett.*, 2002, 1060–1061.
5 Q. H. Li, J. H. Wu, Q. W. Tang, Z. Lan, P. J. Li, J. M. Lin and L. Q. Fan, *Electrochem. Commun.*, 2008, **10**, 1299–1302.
6 K. Imoto, K. Takahashi, T. Yamaguchi, T. Komura, J. Nakamura and K. Murata, *Sol. Energy Mater. Sol. Cells*, 2003, **79**, 459–469.
7 S. I. Cha, B. K. Koo, S. H. Seo and D. Y. Lee, *J. Mater. Chem.*, 2010, **20**, 659–662.
8 J. D. Roy-mayhew, D. J. Bozym, C. Punckt and I. A. Aksay, *ACS Nano*, 2010, **4**, 6203–6211.
9 S. Solar, C. Based, L. Kavan, J. H. Yum and M. Grätzel, *ACS Nano*, 2011, **5**, 165–172.
10 M. K. Wang, A. M. Anghel, B. Marsan, N. C. Ha, N. Pootrakulchote, S. M. Zakeeruddin and M. Grätzel, *J. Am. Chem. Soc.*, 2009, **131**, 15976–15977.
11 H. C. Sun, D. Qin, S. Q. Huang, X. Z. Guo, D. M. Li, Y. H. Luo and Q. B. Meng, *Energy Environ. Sci.*, 2011, **4**, 2630–2637.
12 D. Hwang, H. Lee, S. Y. Jang, S. M. Jo, D. H. Kim, Y. Seo and D. Y. Kim, *ACS Appl. Mater. Interfaces*, 2011, **3**(7), 2719–2725.
13 P. N. Zhu, M. V. Reddy, Y. Z. Wu, S. J. Peng, S. Y. Yang, A. S. Nair, K. P. Loh, B. V. R. Chowdari and S. Ramakrishna, *Chem. Commun.*, 2012, **48**(88), 10865–10867.
14 N. Q. Fu, Y. Y. Fang, Y. D. Duan, X. W. Zhou, X. R. Xiao and Y. Lin, *ACS Nano*, 2012, **6**, 9596–9605.
15 G. Q. Wang and S. P. Zhuo, *Phys. Chem. Chem. Phys.*, 2013, **15**, 13801–13804.
16 X. Y. Zhang, X. Chen, S. M. Dong, Z. H. Liu, X. H. Zhou, J. H. Yao, S. P. Pang, H. X. Xu, Z. Y. Zhang, L. F. Li and G. L. Cui, *J. Mater. Chem.*, 2012, **22**, 6067–6071.
17 F. Gong, H. Wang, X. Xu, G. Zhou and Z.-S. Wang, *J. Am. Chem. Soc.*, 2012, **134**, 10953–10958.
18 J. Yang, C. X. Bao, J. Y. Zhang, T. Yu, H. Huang, Y. L. Wei, H. Gao, G. Fu, J. G. Liu and Z. G. Zou, *Chem. Commun.*, 2013, **49**, 2028–2030.
19 R. Kern, R. Sastrawan, J. Ferber, R. Stangl and J. Luther, *Electrochim. Acta*, 2002, **47**, 4213–4225.
20 Q. Wang, J. Moser and M. Grätzel, *J. Phys. Chem. B*, 2005, **109**, 14945–14953.
21 M. X. Wu, X. Lin, T. H. Wang, J. S. Qiu and T. L. Ma, *Energy Environ. Sci.*, 2011, **4**, 2308–2315.
22 C. X. Bao, H. Huang, J. Yang, H. Gao, T. Yu, J. G. Liu, Y. Zhou, Z. S. Li and Z. G. Zou, *Nanoscale*, 2013, **5**, 4951–4957.
23 M. K. Kashif, M. Nippe, N. W. Duffy, C. M. Forsyth, C. J. Chang, J. R. Long, L. Spiccia and U. Bach, *Angew. Chem., Int. Ed.*, 2013, **52**, 5527–5531.
24 G. G. Xue, Y. Guo, T. Yu, J. Guan, X. R. Yu, J. Y. Zhang, J. G. Liu and Z. G. Zou, *Int. J. Electrochem. Sci.*, 2012, **7**, 1496–1511.
25 M. Grätzel, *C. R. Chim.*, 2006, **9**, 578–583.
26 E. Olsen, G. Hagen and S. E. Lindquist, *Sol. Energy Mater. Sol. Cells*, 2000, **63**, 267–273.

